Unveiling the structural origin of the high carrier mobility of a molecular monolayer on boron nitride

Rui Xu,[1,*] Daowei He,[2,*] Yuhan Zhang,[2] Bing Wu,[2] Fengyuan Liu,[2] Lan Meng,[1] Jun-Fang Liu,[1] Qisheng Wu,[3] Yi Shi,[2] Jinlan Wang,[3] Jia-Cai Nie,[1] Xinran Wang,[2,†] and Lin He[1,‡]

[1]*Department of Physics, Beijing Normal University, Beijing, 100875, People's Republic of China*

[2]*National Laboratory of Solid State Microstructures, School of Electronic Science and Engineering, and Collaborative Innovation Center of Advanced Microstructures, Nanjing University, Nanjing, 210093, People's Republic of China*

[3]*Department of Physics, Southeast University, Nanjing, 211189, People's Republic of China*

(Received 24 September 2014; revised manuscript received 2 December 2014; published 12 December 2014)

Very recently, it was demonstrated that the carrier mobility of a molecular monolayer dioctylbenzothienobenzothiophene (C_8-BTBT) on boron nitride can reach 10 cm^2/Vs, the highest among the previously reported monolayer molecular field-effect transistors. Here we show that the high-quality single crystal of the C_8-BTBT monolayer may be the key origin of the record-high carrier mobility. We discover that the C_8-BTBT molecules prefer layer-by-layer growth on both hexagonal boron nitride and graphene. The flatness of these substrates substantially decreases the C_8-BTBT nucleation density and enables repeatable growth of large-area single crystal of the C_8-BTBT monolayer. Our experimental result indicates that only out-of-plane roughness greater than 0.6 nm of the substrates could induce disturbance in the crystal growth and consequently affect the charge transport. This information would be important in guiding the growth of high-quality epitaxy molecular film.

DOI: 10.1103/PhysRevB.90.224106 PACS number(s): 68.35.bm, 68.37.Ef

I. INTRODUCTION

Organic molecular crystals have many promising applications in electronics and photonics for the characteristics of flexibility, diaphaneity, and low cost [1–8]. However, the low charge carrier mobility blocks the use of the organic molecular crystals in electronic applications [8–18]. The carrier mobility becomes even worse with decreasing the thickness of the organic crystals. One example is that the carrier mobility of monolayer (ML) organic field-effect transistors (OFETs) is only approaching 0.1 cm^2/Vs so far [14], although many methods have been developed to improve it in the past few years. Until very recently, we show that the carrier mobility of dioctylbenzothienobenzothiophene (C_8-BTBT) ML epitaxially grown on boron nitride (BN) could reach as high as 10 cm^2/Vs [19], which is comparable to that of some two-dimensional (2D) atomic crystals, such as MoS_2 [20–22]. This 2D molecular crystal shows great promise for the low-cost and flexible electronics applications.

To fully understand the origin of the high carry mobility of the C_8-BTBT ML, here the structures of the 2D C_8-BTBT crystal were carefully studied using atomic force microscopy (AFM) and cryogenic scanning tunneling microscopy (STM). Our experimental result indicates that the C_8-BTBT molecules prefer to grow layer-by-layer on hexagonal BN and graphene, and it is facile to control the thickness of the C_8-BTBT crystals by adjusting the growth time and temperature. We also demonstrate that only out-of-plane roughness greater than 0.6 nm of the substrates could act as the C_8-BTBT nucleation center. In our experiment, the C_8-BTBT nucleation density is substantially reduced because of the flatness of substrates. This enables us to grow large-area single crystals of the C_8-BTBT layers repeatedly. The large-area single crystal nature of the C_8-BTBT ML reduces disturbances in electronic transport and may be the key reason of the observed record-high carrier mobility.

II. EXPERIMENTAL METHODS

The C_8-BTBT layers were synthesized by heating C_8-BTBT powder to 100–120 °C in a tube furnace under high vacuum. Graphene and BN are ideal substrates for the growth of high-quality molecular film because both of them are atomically flat without dangling bonds. In our experiments, three different substrates, i.e., graphene on SiO_2 (graphene/SiO_2), BN on SiO_2 (BN/SiO_2), and graphene on Cu foil (graphene/Cu), are used to grow the C_8-BTBT layers. The graphene/SiO_2 and BN/SiO_2 are obtained via transferring an exfoliated graphene and BN onto SiO_2 substrate, respectively. Similar observations about the growth mechanism and the structure of the C_8-BTBT layers are obtained on the two different substrates. The graphene/Cu foil is obtained via a traditional chemical vapor deposition (CVD) method [23] (see Supplemental Material [24] for details), and only the C_8-BTBT layers grown on this substrate are further characterized by STM for the requirement of conductivity in the STM measurements. In the growth of C_8-BTBT, the substrate is put a few inches away from the powder. By controlling the heating temperature and duration, high-quality C_8-BTBT layers with different thickness can be observed [19]. Two independent AFM, an Asylum Cypher and a Veeco Multimode 8, were used under ambient condition in this paper. The same result concerning the thickness of C_8-BTBT films is obtained based on the two different AFM systems. The STM system was an ultrahigh vacuum four-probe scanning probe microscope from UNISOKU. All the STM and scanning tunneling spectroscopy (STS) measurements were performed in an ultrahigh vacuum chamber (10^{-10} Torr),

*These authors contributed equally to this work.
†Corresponding author: xrwang@nju.edu.cn
‡Corresponding author: helin@bnu.edu.cn

and all the images were taken in a constant-current scanning mode at liquid-nitrogen temperature. The STM tips were obtained by chemical etching from a wire of Pt (80%) Ir (20%) alloys. Lateral dimensions observed in the STM images were calibrated using a standard graphene lattice. The tunneling spectrum, i.e., the dI/dV-V curve, was carried out with a standard lock-in technique using a 789-Hz alternating current modulation of the bias voltage.

III. EXPERIMENTAL RESULTS AND DISCUSSION

To explore the growth mechanism, we intentionally interrupt the growth of the C_8-BTBT layers to carry out AFM measurements. The C_8-BTBT films are stable against air exposure. Therefore, the frequent interruption and ambient exposure of the sample for characterization do not change the morphologies of the C_8-BTBT layers. Figures 1(a)–1(e) show sequential AFM snapshots of the C_8-BTBT layers grown on graphene/SiO_2 during a 4-minute growth. In our experiment, the C_8-BTBT is observed to grow only on the graphene or BN (see Figs. S1 and S2 in the Supplemental Material [24] for more experimental results) because of very small binding energy between C_8-BTBT and SiO_2. For simplicity, we introduce coverage Θ, which represents thickness of the C_8-BTBT layers, to describe our experimental result. The coverage is expressed in ML units and can be measured from AFM images [14]. For example, if one layer of C_8-BTBT covers 98% of the whole graphene substrate, we obtain the coverage of sample as $\Theta = 0.98$ ML, and we define $\Theta = 1.0$ ML when one layer of C_8-BTBT covers the graphene surface completely. At growth temperature 110 °C, the thickness of sample reaches $\Theta = 1.98$ ML after a 1-minute growth. Then, the initial two layers can be observed on graphene, i.e., the interfacial layer (IL) covers the whole graphene region and the first layer (1L) covers 98% of the whole graphene region [Fig. 1(b) and also see Fig. S3 in the Supplemental Material [24]]. The second layer (2L) begins to nucleate before the completion of the 1L [Fig. 1(c)]. After a 4-minute growth, the 1L covers the whole graphene and the 2L covers almost half of it [Fig. 1(e)]. Our experimental result indicates that the C_8-BTBT grows in a molecularly ordered layer-by-layer fashion on the graphene/SiO_2 [25].

Other samples grown on graphene/SiO_2 and BN/SiO_2 at different temperatures are also investigated; similar morphologies and thickness of the C_8-BTBT layers are obtained (see Figs. S1 and S2 in the Supplemental Material [24] and more data in Ref. [19]), indicating similar microscopic structures and growth mechanism of the C_8-BTBT layers on the two substrates. Figure 1(f) shows schematic structures of the initial three C_8-BTBT layers grown on the graphene/SiO_2 or BN/SiO_2. The thicknesses of the IL, 1L, and 2L on both the substrates are $\Delta h_1 = 0.60 \pm 0.08$ nm, $\Delta h_2 = 1.70 \pm 0.09$ nm, and $\Delta h_3 = 3.00 \pm 0.15$ nm respectively. For $\Theta \geqslant 3.0$ ML, the thickness of each layer is about 3.0 nm, consistent with the c axis length of the primitive cell in the bulk crystal [26–29]. The thickness of 0.6 nm for the IL arises from a new form of molecular packing, as shown subsequently, attributing to the van der Waals (vdW) interaction between

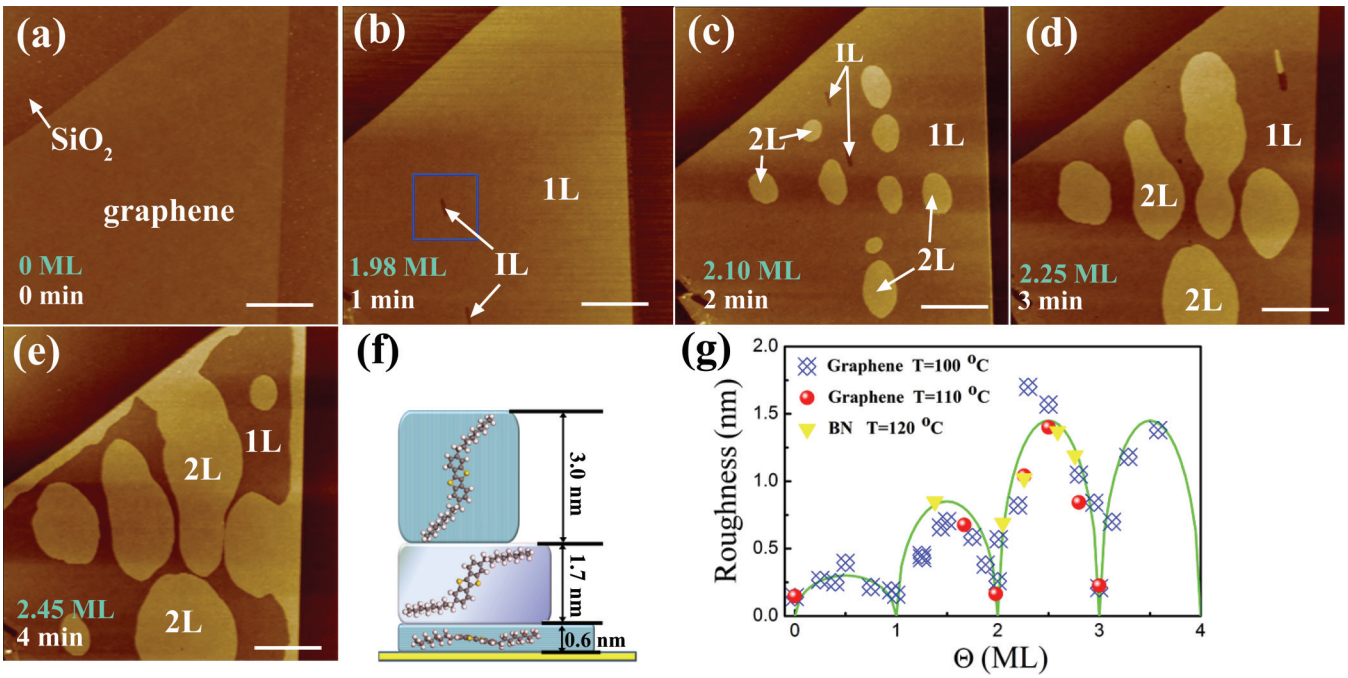

FIG. 1. (Color online) (a)–(e) Sequential AFM snapshots of C_8-BTBT layers on graphene/SiO_2 during a 4-minute growth. The scale bars are 2 μm. The thickness of the molecular film and the duration of growth are marked on each image. (b), (c) Positions indicated by the white arrows and IL are regions only covered by the IL. (f) Schematic diagram of the molecular structure of C_8-BTBT layers on graphene or BN. The thicknesses of the IL, 1L, and 2L on both substrates are 0.60 ± 0.08 nm, 1.70 ± 0.09 nm, and 3.00 ± 0.15 nm, respectively. (g) Roughness of C_8-BTBT layers as a function of the coverage. The green curve is calculated according to Eq. (1). The red solid circles and blue symbols are experimental data on graphene recorded at the growth temperature 110 °C and 100 °C, respectively. The yellow triangles are experimental data of C_8-BTBT layers on BN.

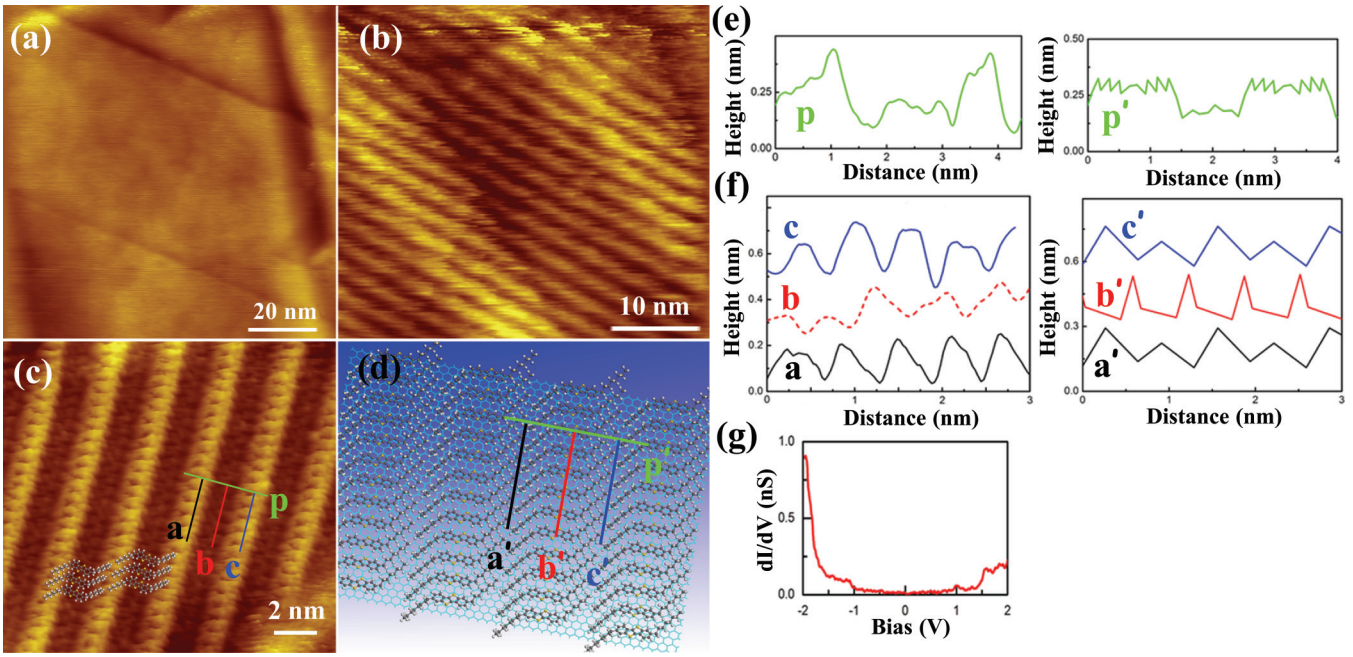

FIG. 2. (Color online) (a) A large-area STM image of graphene surface on Cu foil ($V_{\text{sample}} = -1$ V and $I = 16.8$ pA). (b) A large-area STM image of C_8-BTBT IL ($V_{\text{sample}} = -1.29$ V and $I = 9.08$ pA). (c) A higher magnification STM image of the C_8-BTBT interface layer on graphene/Cu foil ($V_{\text{sample}} = -0.91$ V and $I = 12.1$ pA). The angle between the carbon chains and the benzothiophene is measured to be 140°. The arrangement of molecules is shown in the inset of (c) and (d). Angle between the carbon chains and the benzothiophene is 134°, calculated by DFT. The angle between the benzothiophene plane and the graphene substrate is ~10°. (e) Section lines along the green lines in (c) and (d). (f) Section lines along the lines in (c) and (d). We can see a $\pi/2$ phase ascending from both lines a to c and lines a' to c'. (g) A typical dI/dV-V curve recorded at the IL in Fig. 2(c).

substrates (graphene or BN) and the C_8-BTBT, which allows large lattice mismatch between the substrate and film [30,31]. The vdW forces decay rapidly as r^{-6}; therefore, the role of substrate is much reduced in the 1L and becomes negligible in the 2L and above [32].

To quantitatively understand the growth mechanism of the C_8-BTBT layers, the evolution of the morphology has been further analyzed by means of the surface roughness w, which describes the out-of-plane disorder with respect to the homogeneous layer in a layered morphology. The w is the root mean square fluctuation of the film topography h, and, in layer-by-layer growth, it can be expressed as [14]:

$$w = \sqrt{\langle h^2 \rangle - \langle h \rangle^2} = \Delta h_n [(2n-1)\Theta - n(n-1) - \Theta^2]^{1/2}. \quad (1)$$

Here Δh_n is the thickness of the $(n+1)$th layer (according to our definition, $n = 1$ for IL, $n = 2$ for 1L, and so on). As shown in Fig. 1(g), the roughness w versus coverage Θ measured on both the graphene and BN in our experiment is in good agreement with the predictions of Eq. (1). Therefore, our experimental result demonstrates that the C_8-BTBT molecular crystals prefer layer-by-layer growth for the initial few layers on the two substrates. This result may also be valid for other substrates that are atomically flat without dangling bonds [31].

The structure of the C_8-BTBT layers is further studied by STM measurement. However, only the structure of the IL could be clearly derived from STM images because of limited vertical conductivity of the molecular layers. In our experiment, the IL plays an important role for the observed record-high carry mobility. It not only separates the C_8-BTBT 1L from the influence of the substrate but also becomes the new "substrate" for the growth of the 1L. While carefully controlling the flatness of the substrate, i.e., the graphene on Cu foil [Fig. 2(a)], we successfully synthesize the large-area single-crystal IL, as shown in Fig. 2(b). It is interesting to observe that the growth of the IL is not disturbed by small steps of the substrate. A higher magnification STM image of the IL is shown in Fig. 2(c). The C_8-BTBT molecules are packed in a rectangular lattice with a period of 2.52 nm and 0.66 nm in two orthogonal directions. Based on the observed STM images and density functional theory (DFT) calculations [19], an energy-minimized molecular configuration on graphene is shown in the inset of Fig. 2(c) and Fig. 2(d). Figures 2(e) and 2(f) show the detailed comparison between the structure obtained by STM and the configuration generated by DFT calculation. They agree with each other quite well. Importantly, the thickness of IL obtained by STM measurements and DFT calculation consists well with ~0.6 nm, acquired by AFM experiments. Here, we should point out that the structure of the IL cannot be obtained by cutting along any crystallographic plane of the bulk phase of the C_8-BTBT crystal (see Fig. S4 in the Supplemental Material [24]). Figure 2(g) shows a dI/dV-V curve of the C_8-BTBT IL. The tunneling spectrum reveals a typical semiconducting behavior, which agrees with the fact that the highest occupied molecular orbital-lowest unoccupied molecular orbital (HOMO-LUMO) gap of a C_8-BTBT molecule is about 3.84 eV [33].

To further explore the effect of substrate flatness on the growth of high-quality single crystal molecular layers, we

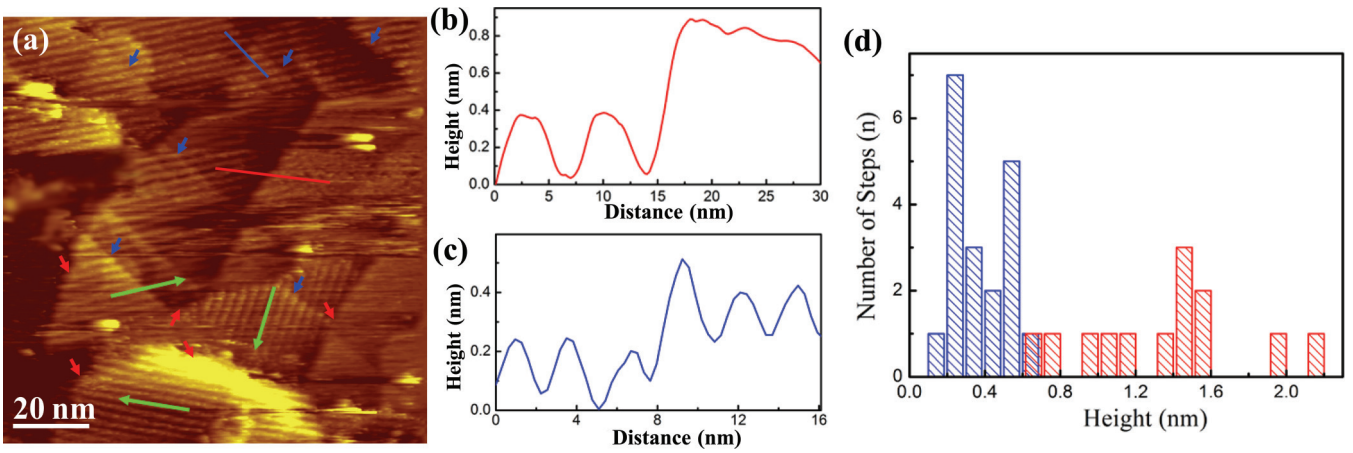

FIG. 3. (Color online) (a) A typical STM image showing multiple domains of the IL ($V_{sample} = 1.04$ V and $I = 10.5$ pA). Green arrows denote the orientations of three different domains. The relative angles between these domains are 21.5°, 98.0°, and 60.5°. The blue and red arrows point to out-of-plane roughness of the substrate. The growth of the IL is disturbed by the out-of-plane roughness, indicated by the red arrows but not by those indicated by the blue arrows. (b), (c)Two typical section lines at the positions of the blue and red lines. (d) Number of steps that do (not) affect the growth of the IL [red bars (blue bars)] versus their height measured in our experiment.

carry out STM measurements of the IL grown on the substrate with large out-of-plane roughness (there are many wrinkles of graphene [23] and large steps of Cu foil). Figure 3(a) shows a typical STM image of our controlled experiment. The large roughness of the substrate induces disturbance on the growth of high-quality C_8-BTBT IL. Small-area domains of the C_8-BTBT IL with different orientations are observed due to the high C_8-BTBT nucleation density induced by the large roughness. The relative angles between these domains usually are not multiples of 60°, which indicates that the C_8-BTBT molecules are not prone to growing along the zigzag or armchair directions of graphene [34–39]. According to our DFT calculation, the maximum difference of binding energy for C_8-BTBT along different directions of graphene is only ~6.8 meV/molecule [19]. The result in Figs. 3(a)–3(c) indicates that the orientation of the C_8-BTBT domain is mainly determined by its nucleation center (for example, the direction of steps in the substrate). Our experimental result also points out that the height of the out-of-plane roughness is a critical parameter that determines the growth of the C_8-BTBT IL, as shown in Fig. 3(d). Only the steps with height larger than 0.6 nm could act as the C_8-BTBT nucleation center. For the substrates of graphene/SiO_2 and BN/SiO_2, the SiO_2 could also induce out-of-plane roughness with height larger than 0.6 nm [40] (also see Fig. S5 in the Supplemental Material [24] for a typical profile line on graphene/SiO_2), which is the nucleation center for the growth of the C_8-BTBT layers. Of course, high-density of such roughness could induce disturbance on the growth of C_8-BTBT IL and is harmful to grow large-area single-crystal C_8-BTBT IL. In our transport measurement [19], we carefully select the substrate and reduce the C_8-BTBT nucleation centers. With successful synthesis of large-area single crystal C_8-BTBT layers, we achieve a record-high charge carrier mobility ~10 cm^2/Vs in the C_8-BTBT 1L. This information is important in guiding the growth of high-quality epitaxy molecular layers.

IV. CONCLUSIONS

In conclusion, the structures of the 2D C_8-BTBT crystals were carefully studied using AFM and cryogenic STM. We demonstrate that the C_8-BTBT molecules prefer to grow layer by layer on graphene and BN, and only out-of-plane roughness greater than 0.6 nm of the substrates could act as the C_8-BTBT nucleation center. The ability to grow high-quality single crystal molecular layers reported in this paper opens the way to the applications in OFETs and is expected to play an important part in future electronics.

ACKNOWLEDGMENTS

We are grateful to the National Key Basic Research Program of China (Grants No. 2014CB920903, No. 2013CBA01603, and No. 2013CBA01604), the National Natural Science Foundation of China (Grants No. 11422430, No. 11374035, No. 11474022, No. 11274154, No. 51172029, No. 61325020, and No. 61261160499), the program for New Century Excellent Talents in University of the Ministry of Education of China (Grant No. NCET-13-0054), the Beijing Higher Education Young Elite Teacher Project (Grant No. YETP0238), and the Fundamental Research Funds for the Central Universities.

[1] H. Sirringhaus, N. Tessler, and R. H. Friend, Science **280**, 1741 (1998).

[2] J. Huang, J. Miragliotta, A. Becknell, and H. E. Katz, J. Am. Chem. Soc. **129**, 9366 (2007).

[3] R. D. Yang, T. Gredig, C. N. Colesniuc, J. Park, I. K. Schuller, W. C. Trogler, and A. C. Kummel, Appl. Phys. Lett. **90**, 263506 (2007).
[4] M. Granstrom, K. Petritsch, A. C. Arias, A. Lux, M. R. Andersson, and R. H. Friend, Nature **395**, 257 (1998).
[5] P. Peumans, S. Uchida, and S. R. Forrest, Nature **425**, 158 (2003).
[6] S. E. Shaheen, C. J. Brabec, N. S. Sariciftci, F. Padinger, T. Fromherz, and J. C. Hummelen, Appl. Phys. Lett. **78**, 841 (2001).
[7] S. R. Forrest, Nature **428**, 911 (2004).
[8] M. Mirza, J.Wang, D. Li, S. A. Arabi, and C. Jiang, Acs Appl. Mater. Interfaces **6**, 5679 (2014).
[9] R. Ruiz, A. Papadimitratos, A. C. Mayer, and G. G. Malliaras, Adv. Mater. **17**, 1795 (2005).
[10] J. Huang, J. Sun, and H. E. Katz, Adv. Mater. **20**, 2567 (2008).
[11] S. Fabiano, C. Musumeci, Z. Chen, A. Scandurra, H. Wang, Y.-L. Loo, A. Facchetti, and B. Pignataro, Adv. Mater. **24**, 951 (2012).
[12] E. C. P. Smits, S. G. J. Mathijssen, P. A. van Hal, S. Setayesh, T. C. T. Geuns, K. A. H. A. Mutsaers, E. Cantatore, H. J. Wondergem, O. Werzer, R. Resel, M. Kemerink, S. Kirchmeyer, A. M. Muzafarov, S. A. Ponomarenko, B. de Boer, P. W. M. Blom, and D. M. de Leeuw, Nature **455**, 956 (2008).
[13] S. G. J. Mathijssen, E. C. P. Smits, P. A. van Hal, H. J. Wondergem, S. A. Ponomarenko, A. Moser, R. Resel, P. A. Bobbert, M. Kemerink, R. A. J. Janssen, and D. M. de Leeuw, Nature Nano. **4**, 674 (2009).
[14] F. Dinelli, M. Murgia, P. Levy, M. Cavallini, F. Biscarini, and D. M. de Leeuw, Phys. Rev. Lett. **92**, 116802 (2004).
[15] Y. Cao, Z. Wei, S. Liu, L. Gan, X. Guo, W. Xu, M. L. Steigerwald, Z. Liu, and D. Zhu, Angew. Chem. **122**, 6463 (2010).
[16] L. Li, P. Gao, W. Wang, K. Mullen, H. Fuchs, and L. Chi, Angew. Chem. Int. Ed. **52**, 12530 (2013).
[17] A. R. Murphy, P. C. Chang, P. V. Dyke, J. Liu, J. M. J. Frechet, V. Subramanian, D. M. DeLongchamp, S. Sambasivan, D. A. Fischer, and E. K. Lin, Chem. Mater. **17**, 6033 (2005).
[18] L. Li, P. Gao, K. C. Schuermann, S. Ostendorp, W. Wang, Ch. Du, Y. Lei, H. Fuchs, L. De Cola, K. Mullen, and L. Chi, J. Am. Chem. Soc. **132**, 8807 (2010). ,
[19] D. He, Y. Zhang, Q. Wu, R. Xu, H. Nan, J. Liu, J. Yao, Z. Wang, S. Yuan, Y. Li, Y. Shi, J. Wang, Z. Ni, L. He, F. Miao, F. Song, H. Xu, K. Watanabe, T. Taniguchi, J.-B. Xu, and Xinran Wang, Nature Commun. **5**, 5162 (2014).
[20] H. Qiu, T. Xu, Z. Wang, W. Ren, H. Nan, Z. Ni, Q. Chen, S. Yuan, F. Miao, F. Song, G. Long, Y. Shi, L. Sun, J. Wang, and X. Wang, Nature Commun. **4**, 2642 (2013).
[21] H. Qiu, L. Pan, Z.Yao, J. Li, Y. Shi, and X. Wang, Appl. Phys. Lett. **100**, 123104 (2012).
[22] H. Liu, M. Si, S. Najmaei, A. T. Neal, Y. Du, P. M. Ajayan, J. Lou, and P. D. Ye, Nano Lett. **13**, 2640 (2013).
[23] K.-K. Bai, Y. Zhou, H. Zheng, L. Meng, H. Peng, Z. Liu, J.-C. Nie, and L. He, Phys. Rev. Lett. **113**, 086102 (2014).
[24] See Supplemental Material at http://link.aps.org/supplemental/10.1103/PhysRevB.90.224106 for more experimental data and details of analysis.
[25] J. B. Gustafsson, H. M. Zhang, and L. S. O. Johansson, Phys. Rev. B **75**, 155414 (2007).
[26] T. Izawa, E. Miyazaki, and K. Takimiya, Adv. Mater. **20**, 3388 (2008).
[27] C. Liu, T. Minari, X. Lu, A. Kumatani, K. Takimiya, and K. Tsukagoshi, Adv. Mater. **23**, 523 (2011).
[28] T. Uemura, Y. Hirose, M. Uno, K. Takimiya, and J. Takeya, Appl. Phys. Express **2**, 111501 (2009).
[29] H. Minemawari, T. Yamada, H. Matsui, J. Tsutsumi, S. Haas, R. Chiba, R. Kumai, and T. Hasegawa, Nature **475**, 364 (2011).
[30] A. Koma, Thin Solid Films **216**, 72 (1992).
[31] A. K. Geim and I. V. Grigorieva, Nature **499**, 419 (2013).
[32] D. Y. Zhong, F. Lin, L. F. Chi, Y. Wang, and H. Fuchs, Phys. Rev. B **71**, 125336 (2005).
[33] H. Kobayashi, N. Kobayashi, S. Hosoi, N. Koshitani, D. Murakami, R. Shirasawa, Y. Kudo, D. Hobara, Y. Tokita, and M. Itabashi, J. Chem. Phys. **139**, 014707 (2013).
[34] Y. Kaneda, M. E. Stawasz, D. L. Sampson, and B. A. Parkinson, Langmuir **17**, 6185 (2001).
[35] M. Linares, L. Scifo, R. Demadrille, P. Brocorens, D. Beljonne, R. Lazzaroni, and B. Grevin, J. Phys. Chem. C **112**, 6850 (2008).
[36] X. Shao, X. Luo, X. Hu, and K. Wu, J. Phys. Chem. B **110**, 15393 (2006).
[37] R. Arai, S. Uemura, M. Irie, and Kenji Matsuda, J. Am. Chem. Soc. **130**, 9371 (2008).
[38] K. Kim, K. E. Plass, and A. J. Matzger, Langmuir **21**, 647 (2005).
[39] M. E. Stawasz and B. A. Parkinson, Langmuir **19**, 10139 (2003).
[40] R. Decker, Y. Wang, V. W. Brar, W. Regan, H.-Z. Tsai, Q. Wu, W. Gannett, A. Zettl, and Michael F. Crommie, Nano Lett. **11**, 2291 (2011).